Original Russian Text: Skryabina N.E., Aptukov V.N., Romanov P.V., Fruchart D. A grid method quantifying deformed Mg-alloys by equal-channel angular pressing. *PNRPU Mechanics Bulletin*, 2015, no. 3, pp. 133-145. DOI: 10.15593/perm.mech/2015.3.10

PNRPU MECHANICS BULLETIN

№ 1-2, 2018

http://vestnik.pstu.ru/mechanics/about/inf/

DOI: 10.15593/perm.mech/eng.2018.1.13
UDC 539.3

GRID METHOD FOR STUDYING DEFORMED MG-ALLOYS BY EQUAL-CHANNEL ANGULAR PRESSING

N.E. Skryabina[1], V.N. Aptukov[1], P.V. Romanov[1], D. Fruchart[2]

[1] Perm State National Research University, Perm, Russian Federation
[2] Institut Néel, 25 rue de Martyrs, Grenoble, France

ARTICLE INFO

Received: 20.06.2014
Accepted: 24.06.2014
Published: 30.06.2018

Keywords:

equal-channel angular pressing, magnesium alloys, grid method, the strain analysis, temperature

ABSTRACT

Metal hydrides are among the optimum solutions for hydrogen storage in terms of effectiveness and safety. Magnesium and its alloys can reversibly absorb hydrogen in large amounts, so according to the DOE's requirements and making those materials attractive for applications. At first, determining a fast hydrogen saturation of Mg-based alloys consisted in grinding the materials up to micrometric grain size. A significant increase of the specific surface of the treated powders by plastic strain processing leads to delivering very reactive samples. Also, huge improvement of H-sorption characteristics of bulk Mg-alloys was shown to be efficient under Equal Channel Angular Pressing (ECAP) treatments. During ECAP treatments, the achievement of a fine grained microstructure in bulk samples is accompanied by the formation of a clear texture.

The main achievements expected from the application of ECAP treatments to Mg-rich alloys are the formation of ultra-fine microstructures with high angle boundaries, which drastically changes the characteristics of the alloy; volume homogenization of the microstructure for the best final stability of the hydrogenation properties of the refined material. Since, in most cases, a two or even more ECAP passes should be applied to deliver highly reacting materials, the operating temperature must be adjusted in terms of ductile to fragile characteristics in order to avoid irreversible cracking of the bulk sample.

After the application of the ECAP process, the resulting strain was characterized using different methods, such as mechanical engineering, numerical simulations and experimental methods. The present article reports on the sample strain process by using the grid evaluation method.

© **Nataliya E. Skryabina** – Doctor of Physical and Mathematical Sciences, Professor, e-mail: natskryabina@mail.ru

Valery N. Aptukov – Doctor of Technical Sciences, Professor, e-mail: aptukov@psu.ru

Petr V. Romanov – Ph. D. Student, e-mail: petr_rom@yahoo.com

D. Fruchart – Research, e-mail: daniel.fruchart@neel.cnrs.fr

1. Introduction

Hydrogen as an energy resource allows to create a closed system of future consumption and conservation of alternative sources of energy (sun, wind, etc.). In addition, hydrogen of high purity is a popular product for the chemical industry. Therefore, the development of elements for renewable storage and transportation of hydrogen is relevant and necessary. Hydrogen is usually stored in liquid or gaseous form. However, extremely high efficiency of the working element (~ 80 %), volume density (150 kg/m^3) and purity (> 99.999 vol. %) of accumulated hydrogen can be simultaneously achieved by hydrogen storage in the form of metal hydrides and alloys. These include magnesium hydride (MgH_2), which is one of the few compounds that meets the standards of the most important hydrogen programs of renewable energy storage systems [1].

The kinetics of magnesium hydride formation is limited by several factors. The main factor is the low rate of hydrogen diffusion in the hydride phase. Hydride nucleations formed on the sample surface at a hydrogen concentration in magnesium x_α < 0,2 at. % [2] overlap, as they increase which does not allow hydrogen to get into a material. Because of this, bulk metals cannot be completely transformed into a hydride. For this purpose, it is necessary to mechanically grind magnesium into powder or (depending on the specific application) to produce magnesium samples in the form of a foil or a thin film.

Authors of the study [3] were able to reveal a positive role of defects and internal stresses in improving the kinetics of sorption/desorption of hydrogen. They proved the advantage of magnesium obtained by mechanical grinding over magnesium obtained by precipitation from the gas phase, particles of which had an almost ideal spherical shape and a smooth surface without any defects.

Fine structure of magnesium can be formed by simple and efficient methods of intensive plastic strain, for example, by equal-channel angular pressing. During ECAP treatments sample goes through a matrix consisting of two channels intersecting at an angle φ (usually angle value φ corresponds to 90, 105 and 120 degrees and varies depending on material plasticity) [4]. Generally stress state of the material depends on the intersection angle of the channels, applied pressure, friction, and presence of counter-pressure. Since the cross section of the sample does not change, strain can be repeated in order to achieve its extremely high degrees (approximately several units).

Under certain conditions, strain of magnesium during ECAP treatments can lead to destruction of the sample. This fact provides a certain perspective for a material preparation for subsequent hydrogen saturation. Even if there were only a partial discontinuity of the sample during ECAP treatments, the subsequent high-energy grinding using planetary mill will come with a significant reduction of time spent on formation of structural state in the material, that can have high reversible hydrogen content. Therefore, conditions and scheme of ECAP treatments should not only the increase length of intergrain and subgrain boundaries in the material, but also create the maximum possible level of micro-stresses in the material, while reducing the tendency to plastic yielding.

It should be considered that during ECAP treatments, depending of deformation conditions (and especially on heating temperature of the matrix), microstructure is formed due to plastic strain and, in some cases, due to (dynamic) recrystallization [5-7].

In the first case, dislocation structure and twin formation have an important role: one can observe glide of dislocations, increase of their density, rearrangement with small-angle boundaries formation, which due to the reconstruction of its structure and partial annihilation of accumulated dislocations are transformed into high-angle boundaries, as the degree of strain increases. In the second case, grain refinement is a result of recrystallization. If the migration of recrystallized grain boundaries into deformed matrix is difficult, the further microstructure evolution is limited by the increase of disorientation between the recrystallized grains and surrounding matrix [8].

It is a well known fact that the occurrence and accumulation of new recrystallized grains in the magnesium structure lead to an increased material plasticity. In terms of necessity of microstructure refinement, this fact is bound to have a negative impact on size reduction of structural elements [9]. However, the results of the published researches [10-14] showed that the initial heating temperature of sample and ECAP matrix, at intersection of which channels plastic strain of the metal occurs, is usually considered as deformation temperature. But a combination of all the conditions of ECAP treatments: strain intensity (angle channels intersection), mode and temperature of passes, as well as speed of sample pass in the channels can have a significant impact on the real sample temperature during intensive plastic strain.

This becomes especially important during ECAP treatments in the range of values close to recrystallization temperature, in which changing is the leading mechanism of microstructure formation.

However, the question of principles of micro-stresses' (or micro-strains) change is still open. According to these principles would allow to determine necessary and sufficient conditions for magnesium deformation during ECAP treatments in order to achieve the required structural state.

2. Materials and Research Methods

Strain of AZ31 alloy samples (96 % Mg, 3 % Al, 1 % Zn, weight %) after a single ECAP treatment at temperatures of 200 and 170 °C was analyzed. The samples in the delivery condition had a form of a parallelepiped with a size of 12×12×50 mm.

Fig. 1 shows the sample surface before ECAP treatment with a mechanically (with a scalpel) applied initial grid with a square cell of 1.95 × 1.95 mm and a depth of not more than 0.1 mm, which does not affect the sample deformation

process. ECAP treatment was carried out in the matrix with the intersection angle of the channels of 105˚ and press punch speed of 3 cm/s.

Before ECAP treatment, a special graphite lubricant was applied to the sample surface in order to reduce friction. However, the applied grid was damaged on some of the samples during the experiments.

Fig. 1. Fragment of the sample surface with an initial grid

Fig. 2 shows the lateral surface of the sample with a deformed grid after ECAP treatment at an initial temperature of 200 °C, and Fig. 3 shows the sample surface after ECAP treatment at an initial temperature of 170 °C. The arrow shows the direction of the sample movement.

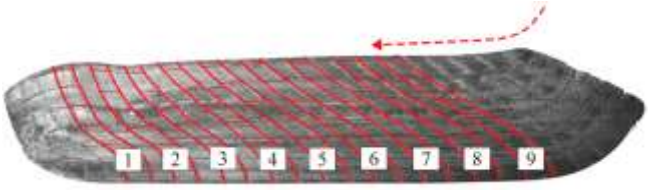

Fig. 2. Sample surface with a deformed grid (T = 200 °C)

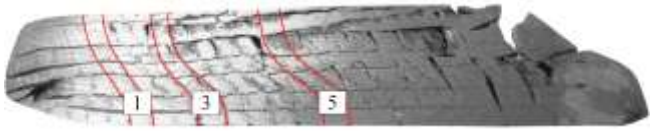

Fig. 3. Sample surface with a deformed grid (T = 170 °C)

As the above mentioned figures show, at the initial temperature of T = 200 °C, the sample stays undamaged and at the temperature of T = 170 °C a lot of cracks occur, especially in tail and top parts of the sample. According to the results of the work [15], during the orthogonal ECAP treatments of magnesium alloy MA2-1 at a speed of 15 mm/min cracks occur at the initial temperature of the sample less than 250 °C.

The direction of the cracks (see Fig. 3) does not match the direction of the deformed grid edges, which makes it very difficult to evaluate strains in the crack formation area.

The following method was used to determine displacement field and increments of strains. The grid method [16] uses initial and deformed grid "freezed-in" with the material or the Lagrangian grid, which is being deformed together with the material. Let us assume that at the n-th stage of strain coordinates of grid nodes x_k^n, y_k^n at the n+1-st stage of strain become coordinates x_k^{n+1}, y_k^{n+1} relative to the current Cartesian coordinate system.

We examine an approximation of the displacement increment field $d\vec{U} = \{dU_x, dU_y\}$ relative to one grid element, going successively across the main movement during the operation of ECAP treatment (see Fig. 4) from the element with nodes 1, 2, 3, 4 to the element with nodes 4, 3, 5, 6.

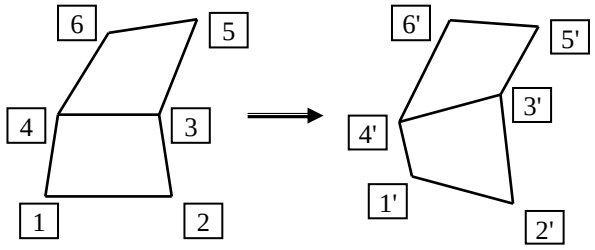

Fig. 4. Pattern of elements at the n-th and n+1-st stage of strain (numbering of grid nodes)

We use a quadratic approximation of displacement field in the selected cells

$$\begin{aligned} \Delta U_x &= A_0 + A_1 x + A_2 y + A_3 xy, \\ \Delta U_y &= B_0 + B_1 x + B_2 y + B_3 xy, \end{aligned} \tag{1}$$

where A_i, B_i are parameters of approximation; $i = \overline{0,3}$.

The coordinates of the grid nodes at the n-th and n+1-st stages are connected with the following formulas:

$$\begin{aligned} x_k^{n+1} &= x_k^n + \Delta U_x\left(x_k^n, y_k^n\right), \\ y_k^{n+1} &= y_k^n + \Delta U_y\left(x_k^n, y_k^n\right), \\ k &= \overline{1,4}. \end{aligned} \tag{2}$$

The formulas (2) are two systems consisting of four linear equations, the total number of unknown variables A_i, B_i is eight.

The components of increment of the Almansi finite strain tensor inside two selected elements, when transferring from the n-th to the $n+1$-st stage are calculated using the formulas [17]

$$\Delta\varepsilon_x = \frac{\partial\left(\Delta U_x\right)}{\partial x} - \frac{1}{2}\left[\left(\frac{\partial\left(\Delta U_x\right)}{\partial x}\right)^2 + \left(\frac{\partial\left(\Delta U_y\right)}{\partial x}\right)^2\right] = \tag{3}$$

$$= A_1 + A_3 y - \ldots - \frac{1}{2}\left[\left(A_1 + A_3 y\right)^2 + \left(B_1 + B_3 y\right)^2\right],$$

$$\Delta\varepsilon_y = \frac{\partial\left(\Delta U_y\right)}{\partial y} - \frac{1}{2}\left[\left(\frac{\partial\left(\Delta U_x\right)}{\partial y}\right)^2 + \left(\frac{\partial\left(\Delta U_y\right)}{\partial y}\right)^2\right] = \tag{4}$$

$$= B_2 + B_3 x - \ldots - \frac{1}{2}\left[\left(A_2 + A_3 x\right)^2 + \left(B_2 + B_3 x\right)^2\right],$$

$$\Delta\varepsilon_{xy} = \frac{1}{2}\left\{\frac{\partial(\Delta U_x)}{\partial y} + \frac{\partial(\Delta U_y)}{\partial x} - \right.$$

$$\left. - \left[\frac{\partial(\Delta U_x)}{\partial x}\frac{\partial(\Delta U_x)}{\partial y} + \frac{\partial(\Delta U_y)}{\partial x}\frac{\partial(\Delta U_y)}{\partial y}\right]\right\} =$$

$$= \frac{1}{2}\{A_2 + A_3 x + B_1 + B_3 y -$$

$$- \left[(A_1 + A_3 y)(A_2 + A_3 x) + (B_1 + B_3 y)(B_2 + B_3 x)\right]\}. \quad (5)$$

In case of a plane strain the strain intensity increment is calculated as follows:

$$\Delta\varepsilon_u = \frac{2}{3}\sqrt{(\Delta\varepsilon_x)^2 + (\Delta\varepsilon_y)^2 - \Delta\varepsilon_x\Delta\varepsilon_y + 3(\Delta\varepsilon_{xy})^2}. \quad (6)$$

Rows of initially vertical cells were treated. Each cell was treated separately: approximation constants of the displacement field were determined by solving the system of equations (2), which resulted in the expressions for components of the finite strain tensor (3)-(5); then the expressions obtained for different cells in one row were brought to a common coordinate system.

3. Results and Discussions

Fig. 5 shows the strain intensity distribution curves for the sample thickness (see Fig. 2) for rows 1 (curve 1), 5 (curve 2), and 8 (curve 3). One can notice an increased strain intensity along the sample from the front part to the tail part, mainly occurring in the central and upper parts of the sample. The maximum level of strain intensity in lateral direction is observed in the central part of the sample. The maximum nonmonotonicity is observed in the front part of the sample. Lateral strain of the sample ε_y and shear strain ε_{xy} contribute the most to the strain intensity. It should be mentioned that uneven strain distribution in the cross section of the sample after ECAP treatments is noted by many researchers, for example [18].

The average value of the achieved strain intensity (see Fig. 5) corresponds to theoretical estimates [19], where ε_u = 78 % (for intersection angle of 105°).

Lateral strain of the sample ε_y is negative, in the middle and upper parts the strain is –90…–45 %, in the lower part it is –30…–15 %.

The strain of cells along the axis of the sample in its middle and tail parts ε_x is positive and in the range of 0-10 %, in the front upper part of the sample there is a compression of up to – 30 %.

Thus, after passing the area of the channel, the intersection velocity of the sample slows down and cells in the front part of the sample are compressed along the movement direction. The main part of the sample (central and rear parts) is exposed to an intense lateral compression strain and shear strain.

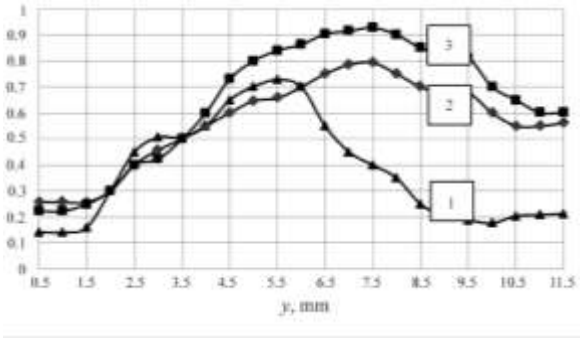

Fig. 5. Strain intensity distribution ε_u over the height of the sample, T = 200 °C

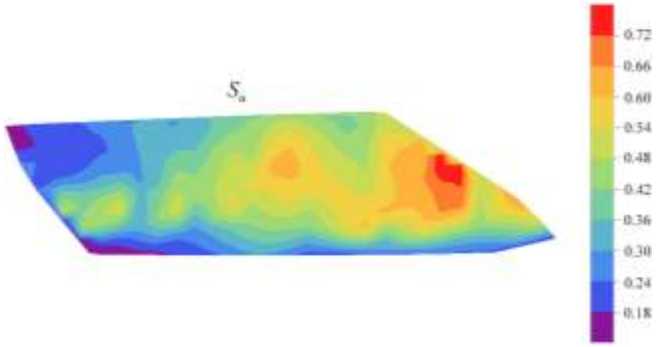

Fig. 6. Strain intensity field on a part of the sample surface, T = 200 °C

Fig. 6 shows the strain intensity field on a part of the sample surface based on the experimental data for separate rows. Severe unevenness indicates the corresponding unevenness of the sample structure obtained during ECAP treatments.

Fig. 7 shows the strain intensity distribution curves across the cracked sample (see Fig. 3) for three selected rows of cells: 1 (curve 1), 3 (curve 2), and 5 (curve 3). In the biggest part of the sample the strain intensity is in the range of 30-40 %, and in the central part it is more than 75 %.

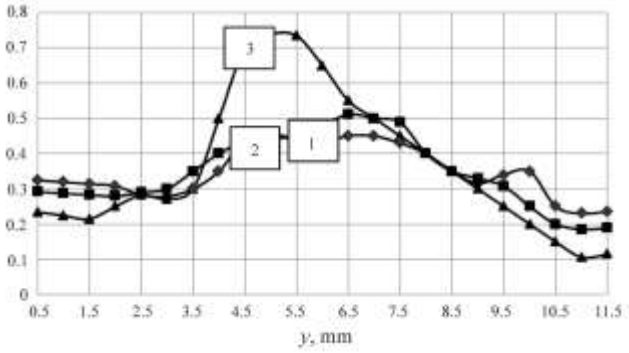

Fig. 7. Strain intensity distribution ε_u over the height of the sample, T = 170 °C

Cracks formation is accompanied by unloading of some sample areas, which limits the strain development and leads to even more uneven strain distribution over the sample

cross section, compared to the strain at a temperature of 200 °C. Cracks formation process depends on the value of critical strain (tensile elongation δ, %) controlled by the initial temperature of the sample. According to the data [20], with an increase of temperature by 50 °C, the tensile elongation of magnesium alloy increases by 25-30 %. Shear strains contribute the most to the strain intensity, just as with a temperature of 200 °C (see Fig. 5).

Thus, the initial temperature of the sample plays an important role in achieving a certain degree of cumulative strain. The purpose of ECAP treatments is to achieve the most homogeneous strain (shear strain intensity) of the sample without cracks formation.

Let us estimate the increase of the sample temperature during intense plastic strain. Energy conservation law in the adiabatic approximation (heat inflow equation) has the following form [21]

$$\rho c \frac{\partial T}{\partial t} = k_T W, \quad (7)$$

where T is temperature; ρ is density; c is the specific thermal capacity; W means work of plastic strain of the material per unit time; k_T is a conversion coefficient of the work of plastic strain into heat.

In terms of increments (assuming that density and specific thermal capacity are constant) the proportion for temperature change has the following form

$$\rho c \Delta T = k_T \Delta W = k_T \int \sigma_u d\varepsilon_u, \quad (8)$$

where $\sigma_u = \left(\frac{3}{2} S_{ij} S_{ij} \right)^{1/2}$ is strain intensity and $\varepsilon_u = \left(\frac{2}{3} e_{ij}^p e_{ij}^p \right)^{1/2}$ is shear strain intensity.

Mises flow rule for isotropic hardening of the loading surface has the following form

$$\sigma_u = \sigma_s \left(\varepsilon_u \right) \quad (9)$$

where $\sigma_s \left(\varepsilon_u \right)$ is the variable yield point of the sample material for tension/compression process (strain curve of the material $\sigma_x = \sigma_x \left(\varepsilon_x \right)$ outside of the elastic limit).

In this case, the value of temperature change during ECAP treatments can be expressed as

$$\Delta T = \left(k_T / \rho c \right) \int \sigma_s \left(\varepsilon_u \right) d\varepsilon_u. \quad (10)$$

A simpler expression for the temperature increase can be obtained in terms of a certain "average" yield point σ_s^{cp} during sample strain

$$\Delta T \approx \left(k_T / \rho c \right) \sigma_s^{cp} \Delta \varepsilon_u . \quad (11)$$

Density of magnesium alloys (ρ) = 1.74 g/cm^3/g = $1.77 \cdot 10^{-5}$ MN·s^2/m^4; specific thermal capacity (c) = = 1.05 kJ/(kg·K) = $1.05 \cdot 10^5$ m^2/(s^2·K).

In works [9, 22], following characteristic values of yield point and strength of AZ31 alloy were obtained during tests of magnesium alloy samples for axial compression before and after ECAP treatments at room temperature: σ_T = 60 MPa, σ_B = 290 MPa. The average value of the cumulative shear strain intensity in the sample according to the experiment (see Fig. 5, T = 200 °C) $\Delta\varepsilon_u$ is 0.55-0.60, the maximum value $\Delta\varepsilon_u$ is 0.72.

For the initial AZ31 alloy at room temperature σ_s^{cp} is 175 MPa. Reduction of the strength characteristics of the alloy for the test temperature T = 200 °C can reach 25 % [20], that is σ_s^{cp} (T = 200 °C) is 131.3 MPa. Value of the conversion coefficient of the work of plastic strain into heat is in the following range: k_T = 0.85–0.95 [23, 24].

With the formula (11) we can determine the value of additional heating of the sample during ECAP treatments: $\Delta T \approx$ 35-40 °C, the maximum heating is $\Delta T \approx$ 43-48 °C. We get similar results for the yield point at room temperature σ_s^{cp} = 175 MPa: $\Delta T \approx$ 44–54 °C, the maximum heating is $\Delta T \approx$ 58–64 °C.

The specified temperature is reached within a very short time, then it drops due to thermal conductivity processes. It should be noted that due to the significant unevenness of the strain distribution over the sample cross section, the local temperature changes can exceed the calculated average values and reach 75–100 °C.

For magnesium alloys the melting temperature (T_p) is 640 °C, and the recrystallization temperature (T_r) is (0.5–0.7) T_p (°K) = 183–257 °C. In some areas of the sample the total temperature may exceed the recrystallization temperature at the initial strain temperature of T = 200 °C and above. In this case, the so-called hot strain mode is carried out along with removing internal stresses.

Thus, the generated heat must be taken into account for the cold strain mode (when total temperature does not exceed the recrystallization temperature) during ECAP treatments.

4. Conclusions

The strain fields in AZ31 magnesium alloy sample were determined by the grid method during a single ECAP treatment at different initial temperatures.

Experiments proved that the strain is rather inhomogeneously distributed over the sample cross section and its average values correspond to the known theoretical estimates.

Lateral strain of the sample and shear strain contribute the most to the plastic strain intensity.

It is shown that the decrease of the initial temperature of the sample from 200 to 170 °C leads to a significant cracks formation and a decreased overall intensity of plastic strains.

Additional heating of the sample during ECAP treatments was theoretically estimated.

It is necessary to take into account both the initial temperature and the additional temperature caused by heat generation during intense plastic strain to control the cold strain mode in order to obtain a specified structure during ECAP treatments.

This work was financially supported by the Ministry of Education of Perm krai, Project No. C-26/211.

References

1. Tarasov B. P., Lototsky B.P., Yartis V.A. Problem of hydrogen storage and perspectives of using of hydrides for hydrogen storage // Ros. Chem. Jour. 2006. Vol. 1, № 6. P. 34-48.

2. Zeng K., Klassen T., Oelerich W., Bormann R. Critical assessment and thermodynamic modeling of Mg-H system // Int. J. Hyd. Energy. 1999. Vol. 24. P. 989-1004.

3. Vigeholm B., Kjøller J., Larsen B., Pedersen A.S. The formation and decomposition of magnesium hydride // J. Less-Common Metals. 1983. Vol. 89. P. 135-144.

4. Valiev R.Z., Langdon T.G. Principles of equal channel angular pressing as a processing tool for grain refinement // Prog. Mat. Sci. 2006. Vol. 51. P. 881-981.

5. Xia K., Wang J.T., Wu X., Chen G., Gurvan M. Equal channel angular pressing of magnesium alloy AZ31 // Mater. Sci. Eng. 2005. Vol. 410. P. 324-327.

6. Yoshida Y., Arai K., Itoh S., Kamado S., Kojyma Y. Realization of high strength and high ductility for AZ61 magnesium alloy by severe warm working // Sci. Tech. Adv. Mater. 2005. Vol. 6. P. 185-194.

7. Estrin Y., Yi S.B., Brokmeier H.-G., Zuberova Z., Yoon S.C., Kim H.S., Hellmig R.J. Microstructure, texture and mechanical properties of the magnesium alloy AZ31 processed by ECAP // Int. J. Mater. Res. 2008. Vol. 99. P. 50-55.

8. Kassner M.E., Barrabes S.R. New developments in geometric dynamic recrystallization // Mater. Sci. Eng. A. 2005. Vols. 410-411. P. 152–155.

9. Skryabina N.E., Aptukov V.N., Romanov P.V., Fruchart D. Impact of equal-channel angular pressing on mechanical behavior and microstructure of magnesium alloy // Bulletin of the Perm National Research University. Mechanics. 2014. № 3. P. 113-128.

10. Skripnyuk V.M., Rabkin E., Estrin Y., Lapovok R. The effect of ball milling and equal channel angular pressing on the hydrogen absorption/desorption properties of Mg–4.95 wt% Zn–0.71 wt% Zr (ZK60) alloy // Acta Materialia, 52 (2004) 405-414.

11. Miyahara Y., Matsubara K., Horita Z., Langdon T.G. Grain refinement and super plasticity in a magnesium alloy processed by equal-channel angular pressing // Metallurgical and Materials Transactions A, 36A (2005) 1705-1711.

12. Estrin Y., Hellming R. Improving the properties of magnesium alloys by equal channel angular pressing // Metal Science and Heat Treatment, 48, № 11-12 (2006) 504-507.

13. Zuberova Z., Kunz L., Lamark T.T., Estrin Y., Janecek M. Fatigue and tensile behavior of cast, hot-rolled, and severely plastically deformed AZ31 magnesium alloy// Metallurgical and Materials Transactions A, 38A (2007) 1934-1940.

14. Figueiredo R.B., Beyerlein I.J., Zhilyaev A.P., Langdon T.G. Evolution of texture in a magnesium alloy processed by ECAP through dies with different angles // Materials Science and Engineering A, 527 (2010) 1709-1718.

15. Kozulin A.A., Skripnyak V.A., Krasnoveikin V.A., Skripnyak V.V., Karavackiy A.K. The study of physical and mechanical properties of ultrafine-grained magnesium alloys after severe plastic deformation // News of higher educational institutions. Physics. 2014. V. 57, N 9. P. 98-104.

16. Del G.D., Novikov N.A. Method of separating grids. M.: Mashinostroenie (Mechanical engineering), 1979.

17. Lurie A.I., Nonlinear theory of elasticity. M.: Nauka, 1980. 520 p.

18. Suglobova I.K., Iliena E.V., Shipachev A.N., Zelepugin S.A. The choice of parameters of loading of titanium samples under dynamic channel-angular pressing // Bulletin of the Tomsk University. Mathematics and mechanics. 2011. N 2(14). P. 111-116.

19. Segal V. M. Slip line solutions for the loading mode and deformation history during equal channel angular extrusion // Materials Science and Engineering A. 2003. V. 345. P. 36-46.

20. Polukhin G.I., Gun G.Ya., Galkin A.M., The Plastic Deformation Resistance of Metals and Alloys. M.: Metallurgy, 1976.

21. Sedov L.I. Continuum mechanics. M.: Nauka, 1973, 536 p.

22. Skriabina N.E., Aptukov V.N., Romanov P.V. Mechanical properties of magnesium alloy samples before and after ECAP // Bulletin of the University of Tambov. Series: Natural and Technical Sciences. 2013, V. 18, № 4. P. 1901-1903.

23. Thomson e.g., Yang, s. Kobayashi, Mechanics of plastic deformation during processing of metals. M.: Mashinostroenie, (Mechanical engineering), 1969.

24. Reznikov A.N. Thermophysics cutting processes. M.: Mashinostroenie (Mechanical engineering), 1970.